Published in: M. Nakagawa and S. Luding (eds.), Powders and Grains 2009: Proceedings of the 6th International Conference on Micromechanics of Granular Media, American Institute of Physics (Melville, New York, 2009), p. 859-862

Fractal Substructures due to Fragmentation and Reagglomeration

D. E. Wolf*, T. Pöschel†, T. Schwager**, A. Weuster* and L. Brendel*

*Department of Physics and CeNIDE, University of Duisburg-Essen, 47048 Duisburg, Germany
†CBI and Center of Excellence EAM, Universität Erlangen-Nürnberg, 91058 Erlangen, Germany
**Charité, Augustenburger Platz 1, 13353 Berlin, Germany

Abstract. Cohesive powders form agglomerates that can be very porous. Hence they are also very fragile. Consider a process of complete fragmentation on a characteristic length scale ℓ, where the fragments are subsequently allowed to settle under gravity. If this fragmentation-reagglomeration cycle is repeated sufficiently often, the powder develops a fractal substructure with robust statistical properties. The structural evolution is discussed for two different models: The first one is an off-lattice model, in which a fragment does not stick to the surface of other fragments that have already settled, but rolls down until it finds a locally stable position. The second one is a simpler lattice model, in which a fragment sticks at first contact with the agglomerate of fragments that have already settled. Results for the fragment size distribution are shown as well. One can distinguish scale invariant dust and fragments of a characteristic size. Their role in the process of structure formation will be addressed.

Keywords: Granular systems,pattern formation,powders,porous materials, fractals macroscopic aggregates
PACS: 45.70.-n,45.70.Qj,61.43.Gt,61.43.Hv

INTRODUCTION

Most particles attract each other, be it by van-der-Waals forces or by microscopic liquid menisci at the contacts, but often this attraction is so weak compared to other forces acting on the particles that it may safely be neglected, when explaining the physical behaviour of granular matter. There are notable exceptions, however, where attractive forces are decisive. In this paper we consider one such case, in which the attractive force between two particles is much larger than their weight. This is true for nanopowders [1], but also for larger particles under microgravity [2], or for wet sand [3].

Such a granular medium with adhesion between the particles can sustain very high porosity in spite of gravity. This can be easily shown: Take two equal glass containers, one empty and the other one at most half filled with dry sand. Porosity is known to be about 0.36 (random dense packing). Then about 10 volume percent of water is kneaded into the sand. One gets a smooth dough. By and by this dough is fragmented by means of a fork into crumbs which are poured into the empty container. One finds the filling height increased. Then the crumb assembly is again fragmented with the fork and filled back into the original container. Again the filling height increases. Repeating this procedure a few times leads to a sand packing with porosity of about 70 percent. Thermophoretic aerosol deposits can even have porosities as high as 99 percent.

In this paper we report on the structural properties of a porous assembly of adhesive particles obtained by repeated fragmentation and reagglomeration. We show that a fractal substructure forms and that the fragment size distribution is very broad. To obtain statistically significant results for the structure one has to consider systems with more than one million particles for many fragmentation-reagglomeration cycles. This is beyond the capability of Molecular Dynamics simulations. Therefore, two simplified two-dimensional models were studied.

The first one, an off-lattice model [4], is a generalization of a model for the sequential deposition of non-adhesive spherical particles under the influence of gravity [5, 6, 7, 8, 9, 10]. The second one is a lattice model, generalizing the model of ballistic deposition [11, 12]. In both models the following procedure is repeated many times: First the agglomerate is cut with a square mesh into portions. The linear mesh size ℓ can be viewed as the typical scale of the fragmentation process. A portion may consist of several disconnected fragments. The models differ in the way these fragments then settle under gravity. They do so as rigid bodies without taking adhesion forces with other particles into account. This is justified, if the flakes are sufficiently large, so that their weight exceeds the adhesive force between the particles. After this reassembly of the fragments the agglomerate is cut again with the square mesh, and so on, see Fig. 1 and Fig. 6. In the following, lengths are given in units of the average particle radius (off-lattice model) respectively the lattice constant (lattice model), masses in units of the particle mass, and time as number of fragmentation-reagglomeration cycles.

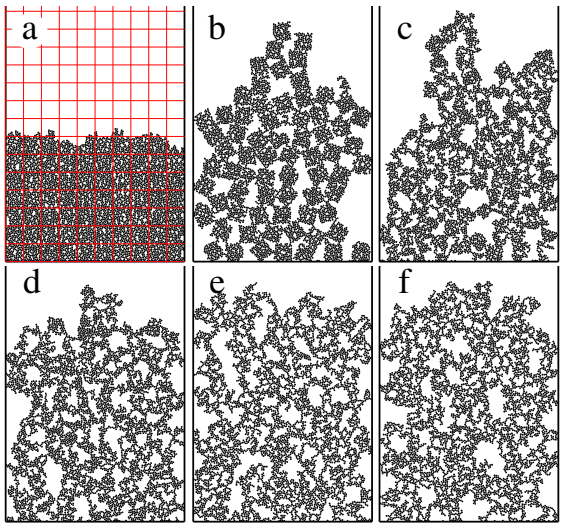

FIGURE 1. Evolution of the packing in the off-lattice model. a) Initial packing generated by random sequential sedimentation [5]. The packing is cut by a square mesh into fragments ($\ell = 20$); b) The fragments are considered as rigid bodies and deposited (1^{st} generation). Again the packing is cut by the square mesh (here not shown); c) the fragments are deposited again (2^{nd} generation), and so on; d) 3^{rd} generation; e) 4^{th} generation; f) 120^{th} generation.

THE OFF-LATTICE MODEL [4]

In this model the reagglomeration of the fragments is simulated in the following way: Each fragment starts at a random position with a random orientation well above the already deposited material (the configuration of which is regarded as frozen in). Following gravity, it moves downwards until it touches the bottom of the container or contacts another already deposited particle. Then it rolls down as a rigid body, again following gravity, until the vertical projection of its center of mass falls in between two points of contact (with the container or previously deposited particles).

We simulated up to 3 million particles represented by discs with a narrow size distribution (10% variance). The initial state was a densely packed agglomerate. In each fragmentation-reagglomeration cycle the filling height increases. Asymptotically, the powder adopts a very porous, statistically invariant structure, which is robust with respect to fragmentation at scale ℓ and subsequent gravitational settling of the fragments.

The filling height h_n at iteration step n approaches the asymptotic height, h_∞, exponentially with a relaxation time, n_0. The inset of Fig. 2 shows that

$$n_0(\ell) \propto \ell^z \quad \text{with} \quad z = 1. \tag{1}$$

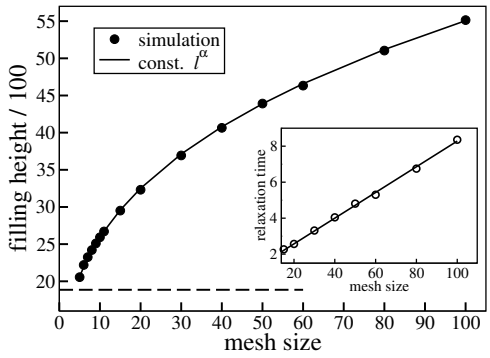

FIGURE 2. The asymptotic filling heigth h_∞ grows as a power law $h_\infty(\ell) \sim \ell^\alpha$ with mesh size ℓ. The full line shows the best fit, $\alpha = 0.327$. Inset: The relaxation time $n_0(\ell)$ increases linearly with mesh size.

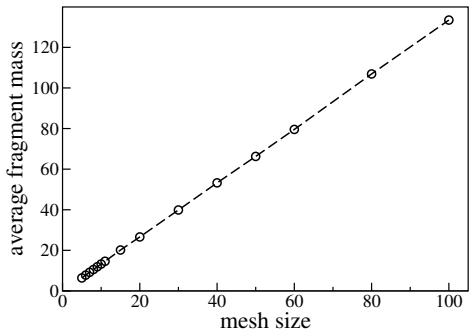

FIGURE 3. Average fragment mass as a function of the mesh size ℓ in the steady state of the off-lattice model.

For the asymptotic filling height, a power law

$$h_\infty(\ell) \propto \ell^\alpha \quad \text{with} \quad \alpha = 0.327 \tag{2}$$

gives a very good fit (see Fig. 2). This implies that the number of portions cut from the steady state configuration of a system of width W scales like $N_\mathrm{p} = h_\infty W/\ell^2 \propto \ell^{\alpha-2}$. Consequently, the mass of a $\ell \times \ell$-portion has a fractal dimension d_f,

$$\frac{M}{N_\mathrm{p}} \propto \ell^{d_\mathrm{f}} \quad \text{with} \quad d_\mathrm{f} = 2 - \alpha = 1.67 \pm 0.03. \tag{3}$$

In the steady state the number of fragments per portion is determined by the fact that the fragmentation process cuts on average as many particle contacts as will be reestablished by the agglomeration process. Since every fragment, when settling, creates two new contacts, the number of fragments per portion must be proportional to the number of contacts cut at the boundary of a mesh cell,

$$\frac{N_\mathrm{f}}{N_\mathrm{p}} \propto \ell^{d_\mathrm{f}-1}. \tag{4}$$

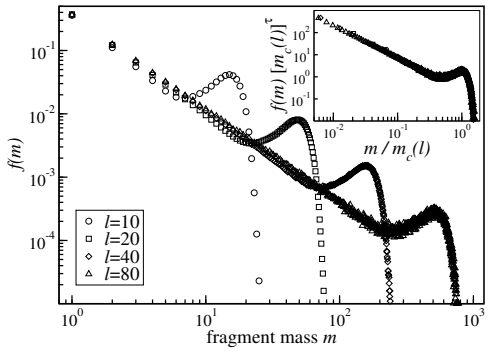

FIGURE 4. Normalized fragment mass distribution for different mesh sizes ℓ. $f(m)$ is the number of fragments of mass m divided by the total number of fragments for a given ℓ. Inset: Data collapse using $m_c \propto \ell^{d_f}$ with $d_f = 1.695$, and $\tau = 1.41$.

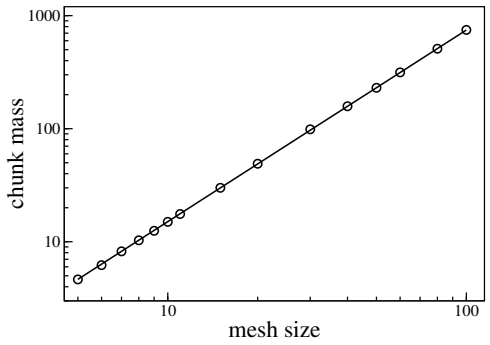

FIGURE 5. Chunk mass m_c as a function of mesh size. Slope of straight line is 1.695.

This is confirmed by Fig. 3, which shows that $M/N_f \propto \ell$.

A detailed understanding of the fragment properties is provided by the distribution of fragment masses, shown in Fig. 4. Two types of fragments must be distinguished, large chunks at the upper end of the mass spectrum with a characteristic size m_c, and scale invariant dust responsible for the power law part that is cut off by m_c. Comparing the mass distributions for different mesh sizes ℓ shows, that they can approximately be written in the form

$$f(m,\ell) = m^{-\tau}\tilde{f}\left(\frac{m}{m_c(\ell)}\right) , \qquad (5)$$

where the scaling function $\tilde{f}(x)$ is constant for $x \ll 1$, goes through a maximum at $x = 1$, and has an approximately Gaussian tail for $x \gg 1$. The typical mass m_c of the chunks has a power-law dependence on the mesh size, $m_c = 0.304\ \ell^{1.695}$ (Fig. 5), the exponent being in good agreement with the value of d_f, Eq. (3).

The fractal chunks are only a tiny fraction of the total number of fragments, N_f. This follows from the fact that the width of the chunk-distribution is proportional to m_c. Therefore, the number of chunks, N_c, divided by the number of fragments, N_f, decreases with increasing mesh size like

$$\frac{N_c}{N_f} \propto m_c^{1-\tau} \propto \ell^{d_f(1-\tau)}. \qquad (6)$$

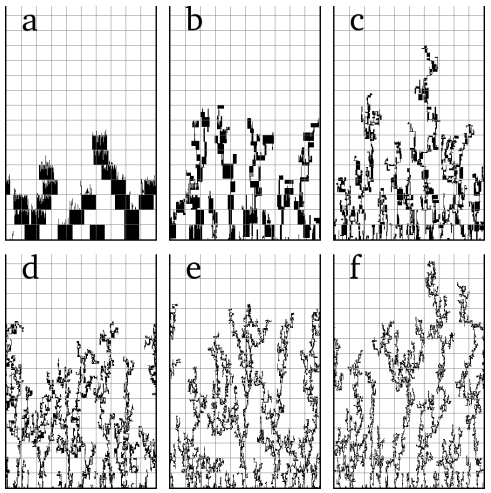

FIGURE 6. Evolution of the packing in the lattice model. a)1^{st} generation. The initial packing was cut by the indicated square mesh into fragments ($\ell = 32$); b) 4^{th} generation; c) 10^{th} generation; d) 20^{th} generation; e) 40^{th} generation; f) 100^{th} generation.

The fractal dimension of the chunks and the dust exponent τ are not independent of each other but obey the scaling relation

$$d_f(2-\tau) = 1 . \qquad (7)$$

The reason is the following: As the chunk mass $m_c \propto \ell^{d_f}$ scales in the same way as the total mass per portion, M/N_p, the number of chunks per portion cannot depend on ℓ. Using (4) and (6) one concludes that

$$\text{const.} = \frac{N_c}{N_p} \propto \ell^{d_f(1-\tau)}\ell^{d_f-1}, \qquad (8)$$

which proves (7). For $d_f = 1.695$ this implies $\tau = 1.41$. These values lead to an excellent data collapse for the fragment mass distributions (see Fig. 4 (inset)).

We have seen, that the overwhelming number of fragments are dust particles, apart from a vanishing fraction (6) of chunks. This explains, why the mass (essentially mass of chunks) per fragment (essentially per dust particle) has nothing to do with the fractal dimension, but is proportional to ℓ (see Fig. 3) .

THE LATTICE MODEL

In order to explore how universal the fractal substructure is, we studied another fragmentation-reagglomeration model. Here all particles live on a square lattice (of width

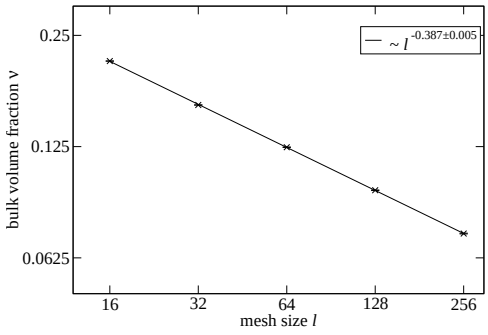

FIGURE 7. The steady state bulk density ν as a function of the mesh size ℓ for the lattice model.

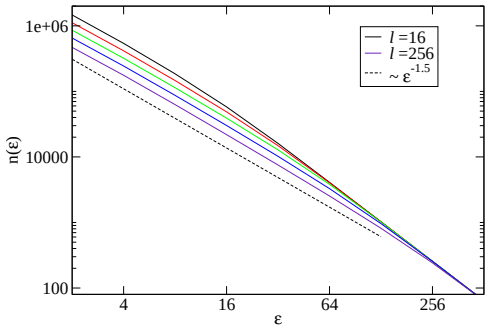

FIGURE 8. The box counting method (ε being the box size) applied to the steady state bulk structure of the lattice model: Below the mesh size ℓ, a fractal dimension of about 1.5 prevails.

W and height H) with lateral periodic boundary conditions, which in each cycle is subdivided into square cells of size $\ell \times \ell$. Then, traversing from bottom to top and each row from left to right, the content of each cell is considered. Disconnected fragments therein are identified and - without changing their orientation - subsequently deposited into an (initially empty) $W \times H$-container at a randomly chosen horizontal position. Deposition means here, that the fragment sinks vertically until it forms the first *vertical* contact with the container bottom or a previously deposited cluster. At this point it stops moving. In contrast to the ballistic deposition model [12] horizontal contacts have no effect for the deposition process, but they become as sticky as any other contact, once the fragment is at rest. As the fragments do not roll down until they form a second contact, the structure, see Fig.6, is more treelike than in Fig.1.

In the following, we show results for a system with $N = 2^{26}$ particles (occupied lattice sites) in a container of width $W = 4096$. The mesh size ranges from $\ell = 16, \ldots, 256$. Data are averaged over 6 independent runs, starting from initial conditions of randomly deposited single particles. As for the off-lattice model the system approaches a steady state in relaxation time $n_0 \propto \ell$, i.e. the exponent z is 1.

Figure 7 shows that the bulk volume fraction ν in the steady state is a power law of the mesh size ℓ with a non-trivial exponent: $\nu \propto \ell^{d_f - 2} = \ell^{-0.387 \pm 0.005}$. This indicates again a fractal substructure up to scale ℓ which is confirmed in Fig.8. The fractal dimension $d_f = 1.5 \pm 0.1$ obtained from the box counting method should be more reliable than the one extracted from the global solid fraction, Fig.7, because of the crossover from the fractal structure on small scales to the homogeneous density on scales larger than ℓ. For the lattice model the fractal dimension seems to be a bit smaller than for the off-lattice model. Lattice anisotropy has a similar effect on the fractal behaviour of DLA [13].

Acknowledgement

We would like to thank I. Goldhirsch for fruitful discussions. This work was partially supported by the German Research Foundation within the collaborative research center SFB 445 “Nanoparticles from the gas phase” and by the German-Israeli Foundation by grant no. I-795-166.10/2003.

REFERENCES

1. L. Mädler, A. A. Lall, and S. K. Friedlander, Nanotechnology **17**, 4783 (2006).
2. J. Blum, G. Wurm, Annu.Rev.Astron.Astr. **46**, 21 (2008).
3. S. Herminghaus, Adv.Phys. **54**, 221 (2005).
4. T. Schwager, D. E. Wolf, and T. Pöschel, Phys. Rev. Lett. **100**, 218002 (2008).
5. W. M. Visscher and M. Bolsterli, Nature **239**, 504 (1972).
6. R. Jullien, P. Meakin, and A. Pavlovitch, Europhys. Lett. **22**, 523 (1993).
7. R. Jullien and P. Meakin, Europhys. Lett. **4**, 1385 (1987).
8. R. Jullien and P. Meakin, Europhys. Lett. **6**, 629 (1988).
9. G. Baumann, E. Jobs, and D. E. Wolf, Fractals **1**, 767 (1993).
10. G. Baumann, I. M. Jánosi, and D. E. Wolf, Phys. Rev. E **51**, 1879 (1995).
11. M. J. Vold, J. Colloid Sci. **14**, 168 (1959).
12. P. Meakin, P. Ramanlal, L. M. Sander, R. C. Ball, Phys. Rev. A **34**, 5091 (1986).
13. P. Meakin, in *Phase Transitions and Critical Phenomena*, edited by C. Domb and J. L. Lebowitz (Academic Press, London, 1988), vol. 12, p.336.